Plasma Modification through Boron Particulate Injection in the full Tungsten Environment of WEST

R. Lunsford[1], A. Gallo[2], K. Afonin[2], Ph. Moreau[2], A. Diallo[1], M. De Combarieu[2], S. Bose[1], D. Sgrelli[2], A. Bortolon[1], C. Bourdelle[2], C. Desgranges[2], A. Ekedahl[2], C. Guillemaut[2], J.P. Gunn[2], C.C. Klepper[3], P. Manas[2], A. Nagy[1], F.-P. Pellissier[2], E. Tsitrone[2], E.A. Unterberg[3], L. Vermare[4], and the WEST Team

[1] *Princeton Plasma Physics Laboratory, Princeton, NJ USA*
[2] *CEA IRFM, F-13108 Saint-Paul-Lez-Durance, France*
[3] *Oak Ridge National Laboratory, Oak Ridge TN, USA*
[4] *Ecole Polytechnique—LPP, Paris, France*

Email: rlunsfor@pppl.gov

ABSTRACT

Recent experiments have confirmed the compatibility of extended boron particulate injections with high performance plasma discharges in the full tungsten (W) environment of WEST. Utilizing an impurity powder dropper(IPD) equipped with boron(B) powders a series of extended experimental programs providing controlled injections have quantified plasma response to varying levels of injection rate and total injection quantity. Calibration of injection quantities confirmed through post-situ testing of the IPD and cross-correlated with both high-speed camera illumination and spectroscopic measurement have allowed for the first time a fine scale determination of the effects of powder introduction on plasma performance. Plasma enhancement, consistent with turbulence reduction through profile modification, has been observed with sustained increases in the stored energy (W_{MHD}), by 18%, electron temperature (T_e) by 35%, and neutron rate (N_n) by up to 200%, all of which scale positively with increasing powder injection rates. These injections have also resulted in both prompt and extended reductions in native impurity content, decreases in post injection radiated power, and strong decreases in divertor deuterium signatures signifying a reduction in recycling suggesting enhanced boron layer formation which provides a reduction of source terms and leads to enhanced gettering of main ion and impurity sources.

I. INTRODUCTION & BACKGROUND

The scalings laws and performance characteristics of a fusion research device are largely determined by the engineering parameters around which the device is constructed. Within the bounds provided by these scalings, enhancement of plasma confinement remains a crucial area of research to ensure optimal performance of the device especially as it pertains to achieving the research mission. The addition of impurities to the edge of the discharge has been one way to affect just such an increase in plasma performance. The JET transition to a full metal wall saw with it a decrease in overall plasma performance[1] however, it was determined that this observed decrease in performance could be recovered through the judicious application of radiative gas injection into the edge of the discharge[2]. Specifically, experiments which introduced nitrogen gas saw the generation of a radiative zone in the divertor and the corresponding recovery of plasma performance. The utilization of solid material injection has also been found to increase plasma performance in a number of devices. The spallation of lithium into TFTR and its subsequent coating of limiter surfaces through the DOLLOP experiments[3] led to enhanced power output, and the introduction of lithium powders on NSTX-U and DIII-D have led to the cessation of ELM activity for the former[4] and the discovery of an enhanced wide pedestal confinement mode[5] for the latter. Recently the introduction of boron containing powders to multiple devices have all shown improvements to confinement, elevated stored energies, or mitigated instability modes. On ASDEX Upgrade [6, 7], initial experiments with B powder injection showed the ability to recondition limiter surfaces allowing access to lower densities and RMP ELM suppression regimes normally accessed right after a boronization. On EAST[8] experiments have been undertaken with both Li and B powder injections, the latter providing access to a quasi-stationary ELM suppressed H-mode operational regime providing particle exhaust without confinement degradation. Similar B and BN experiments performed on LHD[9, 10] have demonstrated evidence of real-time wall conditioning observed during 40s long discharges through increased impurity control and a reduction in the recycling rate. In addition, a reduced turbulence regime was observed during periods of injection leading to increases in the stored energy, as well as the electron and ion temperatures. These measurements are corroborated by pulsed powder injection experiments performed on W7-X[11] which showed a modification of the edge profiles leading to an increased core ion temperature suggesting a reduction in ITG type turbulence. This paper details an

extension of these material injection experiments into the long pulse ITER-like environment provided by the WEST tokamak.

The WEST[12, 13] diverted tokamak has recently upgraded its plasma facing components to a series of actively cooled ITER grade bulk W monoblock divertor cartridges[14] which will facilitate operational pulses over 1300s in length. This also includes an upgraded diagnostic set as described in [15]. During the initial operation of WEST, it was observed that operations in a full W environment bring with it a series of challenges due to high plasma radiative fraction, and thus a set of wall conditioning techniques were adopted to mitigate influx of tungsten and other impurities into the discharge. In addition to baking, used to reduce the water adsorption in the walls, a pair of volume breakdown methodologies were adopted[16]. During Glow Discharge Cleaning (GDC), a volume breakdown is struck in deuterium gas which then will sputter impurities from the walls. During Glow Discharge Boronization(GDB), a helium glow discharge is seeded with a 15% dopant of diborane(B_2D_6) which, once demolecularized and ionized allows the boron to plate out on the walls forming a multi-nanometer coating over the plasma facing surfaces which will inhibit tungsten sputtering while also gettering other impurities. However, we note that these can only be utilized when the superconducting magnets are cycled off and in the case of GDB there are also human hazards as the dopant gas is toxic and pyrophoric. Thus, due to the extended pulse length it was deemed prudent to also include an in-situ conditioning technique which can be actuated during plasma operation.

To that end, the PPPL Impurity Powder Dropper(IPD)[17] was installed on WEST to explore the applicability of intra-discharge real time wall conditioning. Through gravitational injection of sub-150-micron powders into the upper portion of an active research plasma the IPD introduces room temperature particulates which are ablated, thermalized and redeposited throughout the vacuum vessel on high plasma contact surfaces such as limiters and divertors. Full operational details for the IPD are described in ref[18] and briefly summarized here.

The utilization of a quartet of independent vibrational piezoelectric feeder assemblies allows the introduction of multiple species or sizes of particulate materials at variable drop rates. As the voltage to powder throughput calibration is both species specific, and can be affected by outside

influences, as will be discussed, when referring to the IPD excitation level for this experiment we will indicate the control voltage programmed into the IPD control system. This voltage indicates the amplitude of a resonant sine wave generated by the control system which will, after multi-stage amplification, excite the powder feeders. For these experiments the voltage generated by the control system was multiplied by a factor of 4.4x by an Ashly audio amplifier and then further multiplied by another factor of 4.8x by an isolated step-up transformer leading to a gain of just over 20x from the source to the vibrational piezos. Larger excitation voltages lead to enhanced vibrational amplitudes for the piezoelectric feeders and thus a larger powder throughput rate. At present the 4 powder feeders can be operated either independently or in concert to access a range of plasma modification capabilities and surface conditioning objectives. Particle injection sizes can be chosen from a range of 40 – 250 microns at mass flow rates ranging from 2-200 mg/s. While it is possible to attempt injections with material sizes above or below this operational band, reduced laminar flow has been noted for the smaller sizes and enhanced sensitivity to injection rates is observed for larger granule sizes. Various iterations of IPD type systems have been installed on multiple tokamak and stellarator facilities throughout the world[6-10, 19-24] in an effort to quantify the effects of material injections on wall conditions as well as to note the effects on plasma performance observed during injections.

The primary goal of the IPD program on WEST is to utilize the long pulse capabilities of the device to evaluate the applicability of real-time wall conditioning in a full W environment on reactor relevant time scales. It is anticipated that the deposition of low-Z material onto the walls will mitigate W sputtering into the discharge and its subsequent dilution of core fuel, thus moderating radiative losses generated by highly ionized but not fully stripped W ions. The application of a sacrificial boron coating could also lead to a reduction in W first wall erosion, thus extending the effective lifetime of one of the primary capital costs for a reactor system. While acknowledging that considerable engineering concerns need to be addressed prior to large scale adoption of particulate coating techniques, we note that the experiments detailed herein have demonstrated the necessary first steps of operational compatibility and in many cases enhancement of plasma performance coincident with extended powder injections.

II. EXPERIMENT

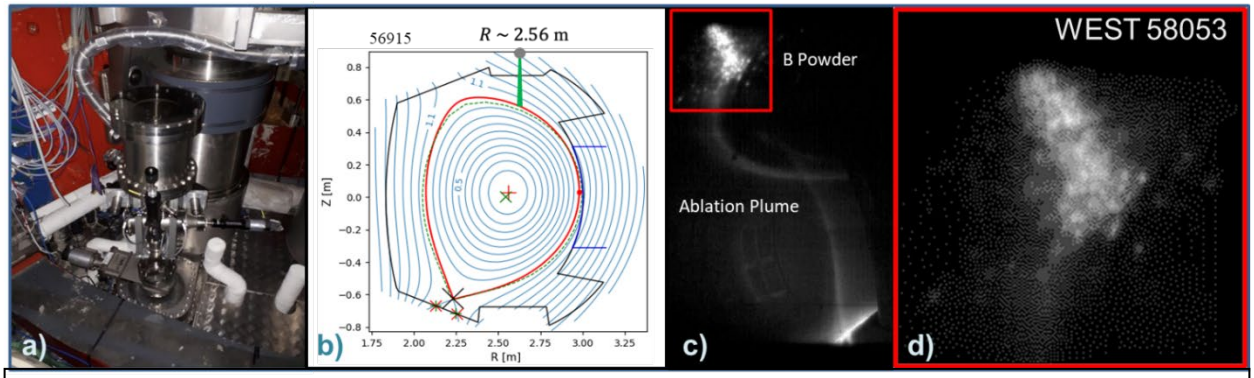

Figure 1: Implementation of the IPD on WEST. Panel a) shows an image of the IPD as installed on WEST while panel b) shows injection geometry for a nominal WEST discharge with the green line indicating injection location. Panel c) shows the results of injection as recorded by WEST camera imaging with panel d) displaying a close up of the powder as it begins to ablate upon contacting the boundary of the discharge.

An IPD was installed on WEST in January 2021 through collaborative effort between PPPL and CEA-IRFM as shown in panel a) of figure 1 with initial commissioning and experimental programs conducted shortly thereafter[16]. Follow on experiments were conducted in March 2023 to better classify plasma response to the introduction of powder and these experiments are discussed herein. Boron powder, of approximately 100-micron diameter, was introduced into the crown of a series of lower single null deuterium discharges as shown in panel b) of figure 1, with the IPD location denoted by the green line intersecting the crown of the discharge. Plasma parameters were held consistent throughout the experiment with I_P = 0.5MA, P_{LHCD} ~ 4MW, B_T = 3.7T, line averaged density $n_{e,0} \sim 4x10^{19}$ m^{-2}, q_{95} = 4.3 and a pulse length of approximately 30s. The injected powder assimilates into the discharge as the particulates are ablated and thermalized, and then distributed through both field parallel transport to the limiter and divertor surfaces as well as perpendicular transport to the first wall, as highlighted by the ablation plume shown in panel c) of figure 1. The material introduced by the IPD was summarily deposited onto the plasma facing components(PFCs) through plasma enhanced vapor deposition as a sacrificial coating. Events occurring prior to the initiation of the IPD experiment, namely an emergency vacuum vent of the diagnostic system led to a destabilization of the IPD calibration. Therefore, the initial IPD

injections were utilized to determine the optimal injection rate. Discharge 58049 was designed to return to the values observed in previous WEST IPD experiments.

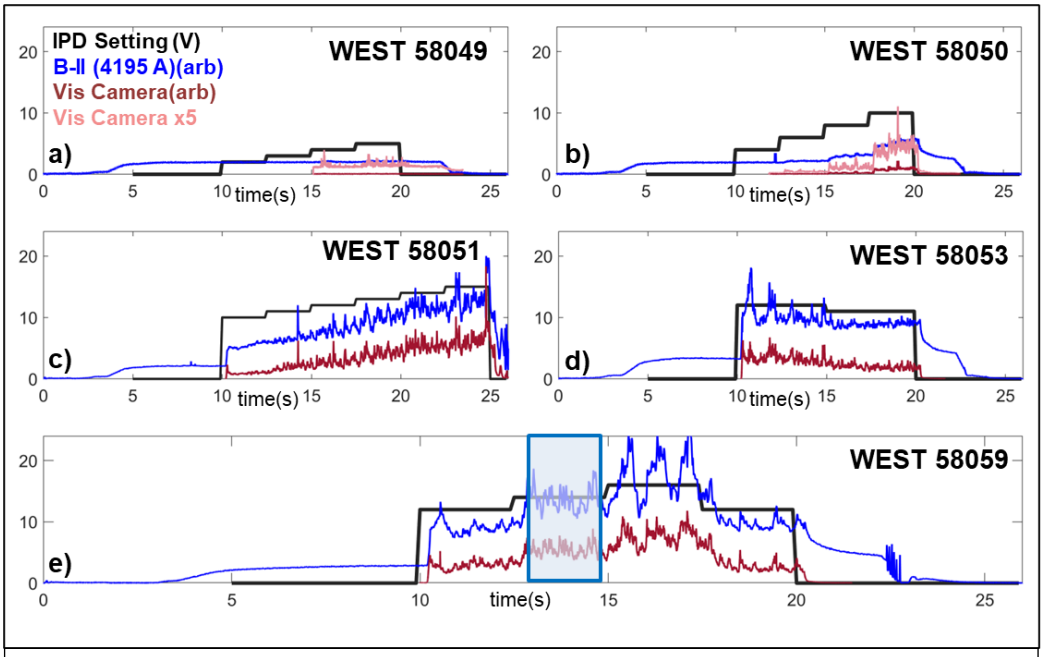

Figure 2: Characterization of boron injection quantities. For each IPD injection discharge in the series the IPD voltage setting is shown in black along with the signal from channel 16 of the lower divertor visible spectroscopy system (shown in blue) as well as the integrated visible camera signal shown in maroon are shown to assist in the quantification of the B powder injection level. Panels a) and b) also show a 5x magnification of the visible camera signal in order to observe the limited quantities of powder injected at these voltage levels.

Observing minimal powder introduction on the high-speed visible camera, the subsequent discharges were utilized as a scan of the available IPD parameter space to reestablish the baseline IPD response. During the experimental session the IPD signal voltage was varied over the course of the flat top portion of the discharge with the applied voltage levels for each discharge recorded in table 1. As shown in figure 2, WEST 58051 was the first discharge with substantial and extended boron injection. This resulted in an observed change in machine conditions as evidenced by the unsuccessful execution of WEST 58052. During this discharge the preprogrammed density ramp was found to be insufficient to reach the target density, most likely due to additional pumping provided by the newly introduced boron and as such the resulting shine through of the lower hybrid heating system led to increased temperatures on vessel components being monitored by the IR protection system. This in turn led to an automated discharge termination by the machine protection system. The plasma program was subsequently modified, allowing WEST 58053 to

run as scheduled. However, during this discharge, the additional introduction of conditioning material led to a further pumping and yet another discharge shutdown by the IR protection system on the next plasma attempt. As such it was decided to run a series of ohmic discharges to reset the machine conditions prior to the execution of the final IPD injection experiment (WEST 58059).

Shot Number	10.0-12.5s	12.5-15.0s	15.0-17.5s	17.5-20.0s	20.0-22.5s	22.5-25.0s
58049	**2V**	**3V**	**4V**	**5V**		
58050	**4V**	**6V**	**8V**	**10V**		
58051	**10V**	**11V**	**12V**	**13V**	**14V**	**15V**
58053	**12V**	**12V**	**11V**	**11V**		
58059	**12V**	**14V**	**16V**	**12V**		

Table 1 : IPD voltage settings for B powder injection shot series

III. QUANTIFICATION OF BORON PARTICULATE INJECTION

A rapid unscheduled ingress of air into the IPD chamber through the WEST diagnostic vacuum system mobilized parts and powder within the IPD system and lead to a destabilization of the IPD calibration. Thus, careful consideration needed to be applied to correlate the settings on the IPD system with the injected powder quantity. To assure reliable quantification of the injection amount a multi-pronged approach was adopted. Powder injection was experimentally verified by fast visible camera observation of the injection site. A region of interest around the injection site, denoted by the box shown in panel c) of figure 1 and expanded in panel d), was integrated frame by frame over the course of the injection. The results of this analysis for each injection program can be seen in the maroon and rose traces seen in panels a)-e) of figure 2, with the maroon trace being the normalized signal and the rose data trace a magnification of that signal for discharges where the injection level was small to moderate in order to show detail. The integrated camera

illumination is then compared to the spectroscopic observation of singly ionized boron recorded at the lower divertor, indicating material that has been ablated, ionized, and transported from the top to the bottom of the plasma, as indicated by the blue traces in the respective panels of figure 2. Noting that this signal decays rapidly after the cessation of injection we are confident that the majority of the contribution is from the newly introduced B powder. The other signal utilized during the calibration was observation of the 419.5 nm B-II spectroscopy line, as monitored at the lower outer divertor. Specifically, spectroscopy line of sight DVIS2-16 (Data Name: 'LODIVOU18') which is located at major radius r = 2.257m and denoted later in this paper by the "OSP" (Outer Strike Point) arrow in figure 12. The line of sight for this chord can be found in Figure 3 of Ref [25]was chosen primarily because it displayed the strongest boron signal. This line of sight is physically located in the middle of the lower outer divertor, coincident with the plasma outer strike point. We note here that as a qualitative diagnostic, the camera signal does not contain an intrinsic absolute timebase. Thus, as part of the processing, the timing of the camera trace was shifted to match that of the spectroscopy signal by utilizing common signal features for alignment. This method was chosen so as to facilitate comparison of the relative signal levels during the injection periods; however, this now means that the initiation of the boron signals, or any delay between the visible and spectroscopic signals cannot be used to determine the transit time of the material between the upper and lower portions of the discharge.

As seen in figure 2, once a minimum IPD control voltage level has been achieved, indicating a minimum effective excitation level for the piezoelectric vibration stage within the IPD, stepwise increases to the IPD control voltage are strongly correlated to an increased delivery of powder as evidenced by both the camera response as well as elevated spectroscopic signals across all injection levels. We also note that increasing levels of powder injection have larger variations within the drop period possibly indicating nonlinear effects within the feeder response. To determine an injection quantity resultant from the voltage application settings, the camera and spectroscopy signals were averaged over each selected voltage level for the central 2 seconds of the drop time. For example, during WEST discharge 58059, as shown in the highlighted section of panel e) within

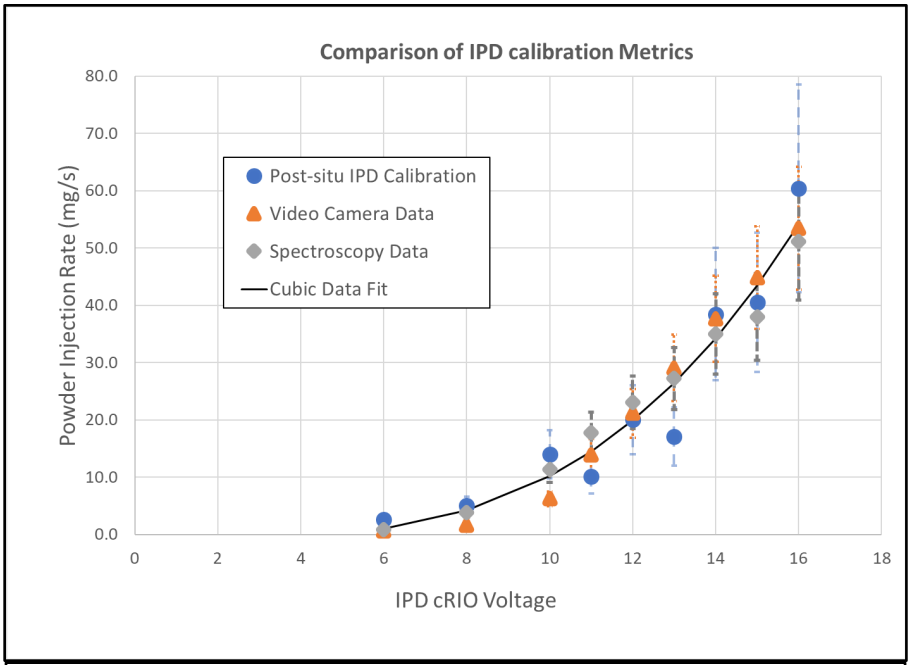

Figure 3: Comparison of IPD calibration metrics. The averaged signals from the high-speed video camera data and spectroscopy measurements are normalized and benchmarked by a post campaign IPD calibration. Error bars represent standard deviation of the measurement for each technique. A fit to the full data set is included to guide the eye and is used to approximate the injection quantity delivered for each IPD voltage setting.

figure 2, an IPD setting of 14V was applied during the time period from 12.5 – 15s. The central 2s of this time period was selected to avoid any carryover effects from the transition between voltage levels, and the visible and spectroscopy signals were averaged to arrive at a value representative of the IPD voltage selection level. As the major plasma parameters were held constant during the flat top portion of each discharge over the experimental series, this method provides a way to determine proportional powder fluence delivered across the injection levels. Since these optical methods only provide a relative calibration immediately following the conclusion of the WEST Spring 2023 campaign, an extensive practical calibration effort was undertaken with the IPD held in as similar a state to the experiments as was possible. For this physical calibration multiple measurements were taken at each voltage with IPD pulses at each voltage lasting longer than 10s. The powder was collected and weighed after each pulse, a throughput per second was calculated, and an average was determined for each voltage. The values obtained from this post-situ calibration were then compared to the optical measurements to ensure that the dropper behaved consistently between the experiment and the calibration activity. To

accomplish this the average injection quantity for each time period, as determined for both the visible camera and spectroscopy data, was normalized to the post situ calibration to corroborate the measurement and the resulting calibration curve utilizing these three methods is displayed in figure 3. As seen, there is strong agreement between the three methods as to the variations in powder injection quantity observed at increased control voltages. An empirical fit to the data (Eq 1) was utilized to determine an approximate powder injection quantity in mg/s for a given voltage(V) and the resultant values as well as the approximate cumulative injection amount are displayed in table 2. This powder injection value is then applied to the remainder of the analysis to quantify the plasma reaction to material introduction.

$$(1) \qquad Drop\ Rate\left(^{mg}/_{s}\right) = 0.0185 * V^3 - 0.0861 * V^2 + 0.0269 * V$$

Shot Number	Average Injection Rate (mg/s)							Approximate Cumulative Injection Quantity (mg)
	10-12.5s	12.5-15s	15-17.5s	17.5-20s	20-22.5s	22.5-25s		
WEST 58049	0	0	0	0.5				1.25
WEST 58050	0	1	4	10				40
WEST 58051	10	14	20	27	35	43		410
WEST 58053	20	20	14	14				580
WEST 58059	20	34	54	20				900

Table 2 : Calculated average injection quantities for the WEST impurity powder dropper experimental series. We note that due to an estimated 300ms drop time of the injected powder, as well as the stochastic transit process through the drop tube, transitions between powder levels are not instantaneous and thus the values given are to be treated as averages over the injection period.

IV. PLASMA RESPONSE TO PARTICULATE INJECTION

The introduction of particulate conditioning materials into the edge of the plasma discharge can substantially modify the plasma performance. A summary of the most prominent prompt effects on the WEST plasma is shown in figure 4. We first note that the injected lower hybrid power at 4MW and plasma current at 500kA, as shown in panel a), was held stable across the entire experimental data set. This was done to facilitate comparisons between different discharge subsections across the experimental series. The IPD injection waveform for WEST 58051 is displayed as the black trace in panel a) and corresponds to the values enumerated in table 1. This level is the voltage setting applied by the control system to the IPD and is utilized to determine the quantity of powder delivered at any given time by the IPD. As shown previously in figure 3, there is a direct correlation between the control signal voltage and powder delivery rate, and as noted in figure 4, these increased rates have a substantial impact upon the discharge. Plasma density, shown in panel b), was controlled by automated gas feedback and was able to maintain, without difficulty, the density setpoint despite the increasing levels of additional mass being injected by the IPD into the discharge. As shown in panel b), the gas puff rate initially decreases as new material is assimilated into the discharge. However, after the initial drop, the gas injection rate begins to rise and continues to ramp upward throughout the remainder of the discharge despite increased B injection. We posit that this could be indicative of increased gettering of the main ion species by the newly deposited boron layer thus causing a substantial reduction in recycling.

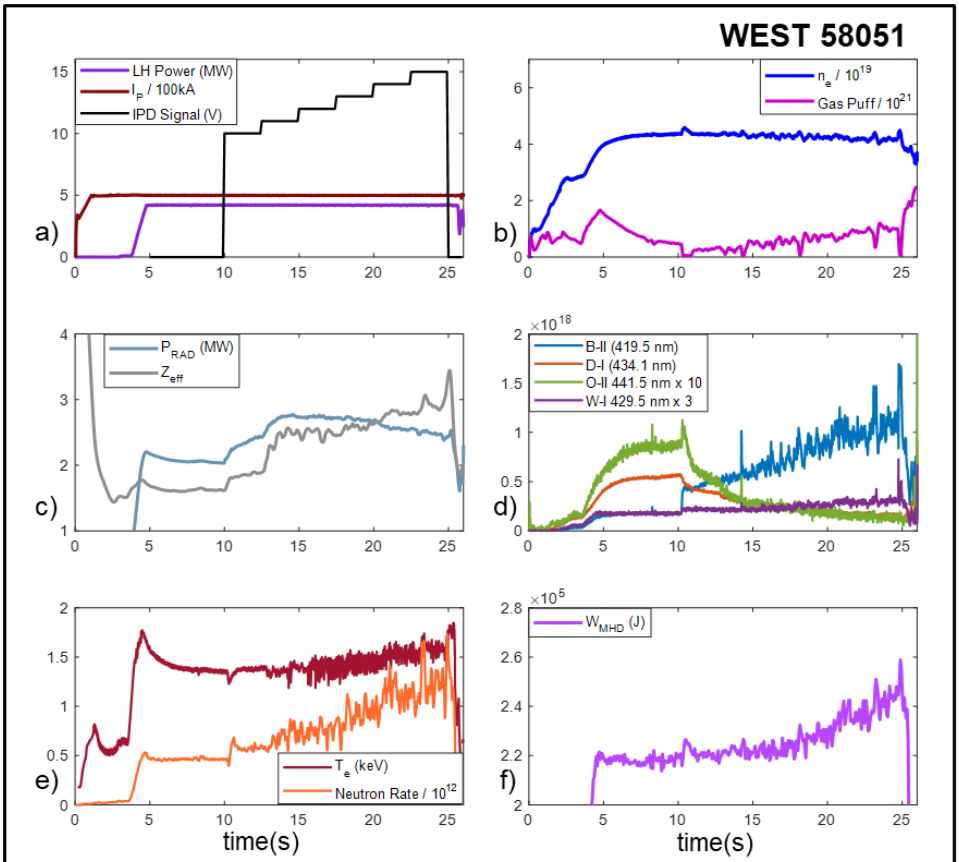

Figure 4: Plasma performance and injection response. Typical responses of plasma parameters to impurity powder injection are shown in the above subpanels. Powder injection is coincident with the IPD control signal as seen in panel a) and approximate powder injection rate in mg/s can be obtained by comparing the IPD control signal to the calibration curve in figure 3.

The introduction of B powder also causes an increase in radiated power, as shown in panel c), however the radiated power appears to roll over and begins to decrease even though the quantity of injected powder is still increasing as evidenced by the continued rise in the spectroscopic B trace in as shown panel d). We also note a mild increase to tungsten signal level, most likely due to increased sputtering by the heavier boron atoms, as well as decreases to deuterium and oxygen signals, which are interpreted as supportive evidence for increased conditioning and explored further in Ref[26]. The introduction of boron powder also leads to multiple indicators of increased plasma performance. As can be seen in panels e) and f), the electron temperature, neutron rate (here being used as a proxy for ion temperature) and the stored energy all are observed to increase

with the introduction of powder. The increases are also observed to vary proportionally with the boron powder injection level and were seen at varying intensities with the other powder injection discharges as well. The remainder of this section examines in turn the modifications to the plasma behavior and performance observed throughout the range of B injection levels.

IV.1 Elevated plasma performance metrics T_e, N_n and W_{MHD}

To classify the average elevation to performance resultant from impurity injection a similar methodology to the determination of powder injection quantity was utilized. Namely, the central two seconds for each drop period was averaged for the respective quantity thus allowing us to categorize the responses of the core T_e, W_{MHD}, and N_n to variable quantities of injected powder. The results of this measurement can be seen in figure 5. For each of the observables we note that small non-perturbative amounts of injected material have either no or mild negative consequences. For T_e, as shown in the top panel, this drop corresponds to approximately half a percent. This is understandable as part of the energy budget is now being dedicated to the ablation and ionization of new material. However, once this non-perturbative limit has been crossed, larger injections lead to increases in the core T_e above a baseline pre-injection temperature of 1.22keV to an average of 1.66keV and a peak value of 1.83keV. Similar increases are also seen in the stored energy (middle panel). Again, a decrease is seen for smaller injection rates however, at the larger rates we note that the average stored energy is now 267kJ (286kJ peak), a noted increase over the baseline level of 228kJ. The bottom panel displays the behavior of the neutron flux rate, again observed to increase with increasing powder mass flow rates. Over the series of injections, we observe a rise in the neutron flux rate from a pre-injection average baseline rate of 4.68×10^{11} s^{-1} to an average of 1.46×10^{12} s^{-1} with a peak of 1.95×10^{12} s^{-1}. This substantial increase is even more striking when one considers that the larger levels of boron introduced at constant plasma n_e means a greater fraction of main ion dilution. For the largest injection rates, Z_{eff} increases to just over 3.1 which corresponds to a charge balance where half of the electron budget is resultant from the impurity inclusion. As such, we are observing an elevated neutron flux rate at substantially reduced main ion densities.

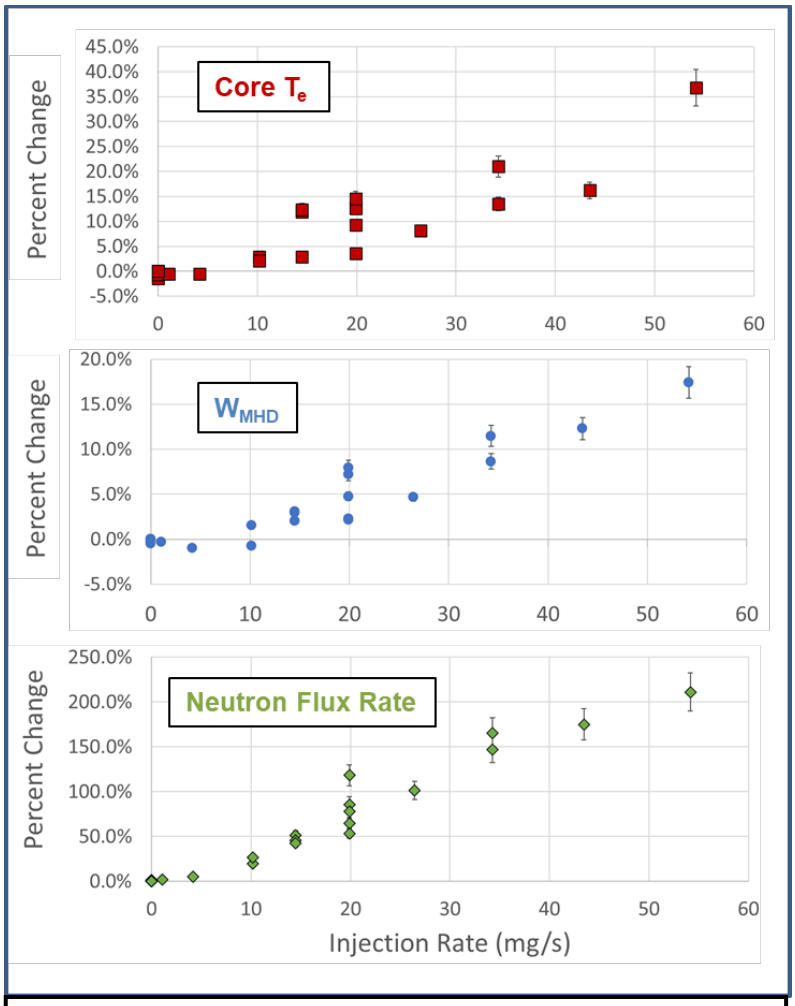

Figure 5 : Scaling of plasma performance with injection quantity. Percent changes are calculated by comparing the average value of the noted plasma metrics vs. those observed during pre-drop phases within the same discharge. Error bars represent the standard deviation of the measurement during the period of averaging.

The foundational cause behind the improvements to WEST performance as a result of powder injection appears to be consistent with those observed in earlier experiments and on other fusion research devices. As is detailed in [23] the increase in electron temperature on WEST is complemented by a broadening of the T_e profile as measured by the ECE diagnostic and accompanying reflectometry profiles. They show an expected increase in density during the initial drop phase, with a corresponding reduction in edge electron temperature reflecting the new energy burden presented by the ablation and thermalization of the new material. These counterbalancing

effects keep the electron pressure approximately constant. In experiments performed on W7-X[11], pulsed injections of Boron Carbide(B_4C) also lead to a steepening of the density profile and thus a reduction in the normalized inverse gradient scale length. These conditions are unfavorable to Ion Temperature Gradient(ITG) type instabilities and lead to a reduction in anomalous transport levels. The reduced anomalous transport leads to observed enhancements in confinement which provides a greater electron-ion collisional interaction time which is most likely responsible for the elevated core ion temperatures despite the purely electron heating being delivered by the ECRH system. Measurements of radially resolved density fluctuations by the Doppler Reflectometer on W7-X have also confirmed a reduction in the presence of turbulent microstructures within the plasma during the injection period. Further evidence of turbulence suppression was observed in LHD[10] after boron powder injection through beam emission spectroscopy and phase-contrast imaging measurements, showing a roughly 50% reduction in density fluctuations across the majority of the plasma radius. The suppression was most pronounced at low frequencies (<50 kHz) associated with drift-wave turbulence, while higher-frequency modes (100–200 kHz) became more prominent, a shift consistent with reduced transport. The effect was reproducible across discharges and robust under both varied heating methods and alternating magnetic configurations thus demonstrating a repeatable turbulence-mitigation mechanism causally linked to boron powder injection. These observations are consistent with the recently conducted experiments on WEST and further analysis and confirmation of the nascent cause of these performance boosts in WEST is ongoing.

That being said, we can see preliminary evidence of the generation of these modifications and their resilience in the temporal evolution of the electron temperature. As shown in panel b) of figure 6 the initial integration of new material at t = 10s drop causes reduction in electron temperature as the free streaming electron channel is depleted by the ablation and ionization

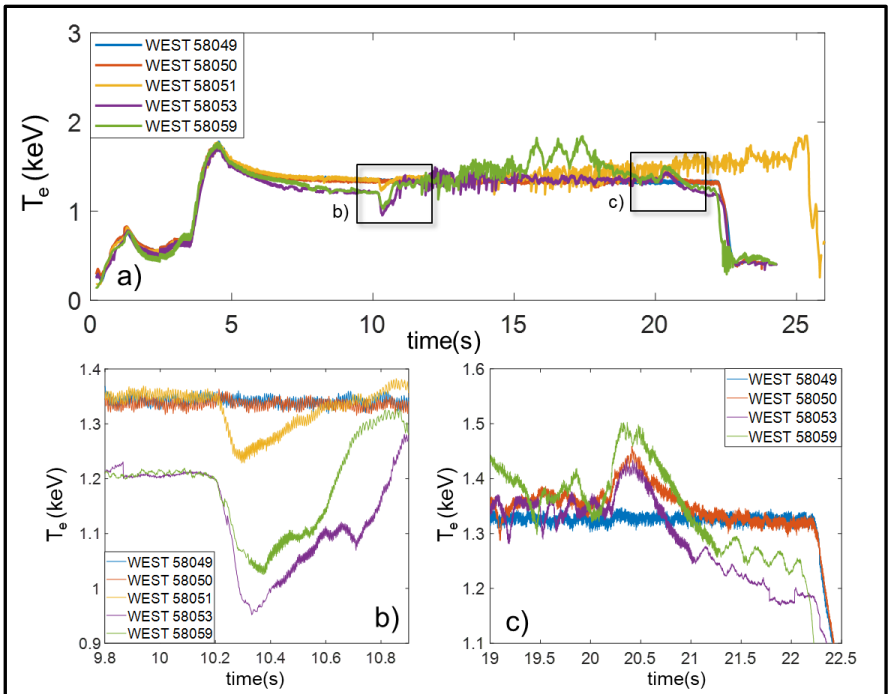

Figure 6 : Evolution of the electron temperature in response to powder injection. In each case powder injection starts at shortly after 10s. Subpanels b) and c) are magnifications of the relevant times in the main panel a). WEST 58051 has been removed from panel c) as the powder injection was still underway at t = 20s and this shot was not terminated at the same time as the other discharges. We also note that WEST 58053 and 58059 have lower initial electron temperatures due to a modification of the baseline discharge parameters in response to the modified machine conditions.

activity. For discharges 58051, 58053 and 58059 which started with strong injection activity the temperature is observed to drop rapidly over the course of 100- 150 ms and then spends the next 600-800 ms rebounding to a level higher than the previous baseline temperature with larger drop rates leading to larger downward excursions and extended recovery times. However, once this transition period has been completed the elevated electron temperature is maintained for the duration of the drop time as can be seen in panel a) of the same figure. Once the injection period has been completed, we observe a post-injection temperature bounce on the discharges with powder injection as seen in panel c). This bounce can be as much as a 15% increase over the temperature observed immediately prior to the injection being concluded. We postulate that this is the result of the rigidity of the temperature profile allowing elevated core temperatures while the

energy loss from the injection burden has been removed. We also note that the drops in 58053 and 58059 temperature levels below the baseline established during 58049, which contained essentially no injection, are a result of these discharges returning to the pre-injection levels observed earlier in the shot and not a degradation to a lower temperature plateau. WEST 58051 also displays the initial drop in temperature upon introduction of powder. This discharge was preprogrammed with a longer duration and so it does not show the post-drop bounce at t = 20s evidenced by the other shots as the powder injection was still going on. Instead, the post drop bounce is shifted to just after t = 25s as shown by the gold trace in panel a). The other differentiating characteristic for this discharge is that the drop rate at the conclusion of WEST 58051 was more than twice the amount injected during the other discharges thus causing a larger elevation above the baseline discharge performance.

IV.2 Modifications to Z_{eff} with B powder injection

Injection of impurities into the discharge also changes the effective ion charge in multiple ways. The first is through fuel dilution as the newly introduced material replaces the Deuterium main ions within the plasma. The second is through an enhanced sputtering of the wall materials by the heavier B atoms. Thus, as can be seen in panel a) of figure 7 there is a rapid increase in Z_{eff} once substantial material throughput begins. For WEST 58050 this means that the appreciable rise does not occur until 17.5s as the dropper rate reaches 10mg/s. In WEST 58051 the initial rise in Z_{eff} during the start of powder injection is similar to what was observed at the end of WEST 58050, but then a sharp jump from 1.9 to 2.5 occurs at 12.5s despite only a moderate increase in boron powder injection level from 10 to 14mg/s. The sharp initial features seen at the beginning of the injections for WEST 58053 and WEST 58059 are believed to be due to the elevated injection rates from the previous IPD experimental discharges. As described in [18], the impurity powder dropper has a small but non-negligible ramp where powder is transported from the storage reservoir to the drop tube. The layer thickness of the transported powder is proportional to the excitation voltage of the IPD and as such these first injection quantities are more likely due to the elevated layer thickness from the previous discharges where the dropper was deployed.

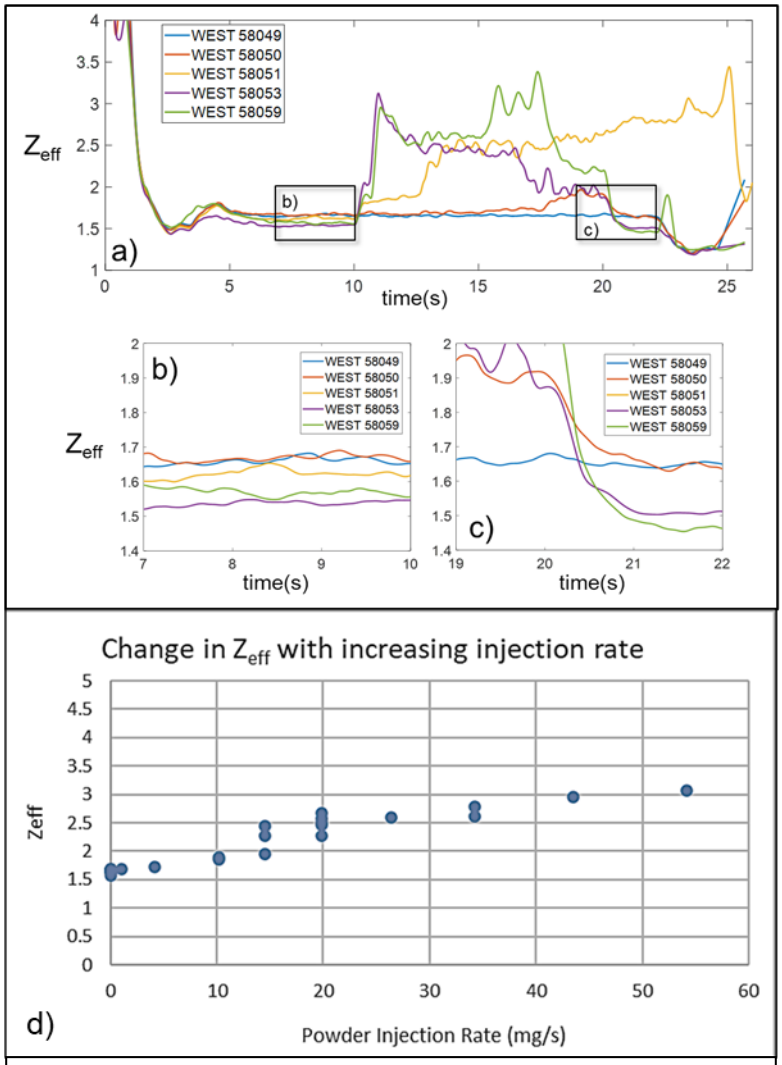

Figure 7 : Modifications to Z_{eff} with varying powder injection rates. Average Z_{eff} for each injection rate determined in a similar manner to other powder affected quantities as previously described.

However, there are additional effects, as panels b) and c) from figure 7 display the cumulative conditioning effect provided by the boron powder injections. As shown in panel b), which displays the pre-injection period, the introduction of boron containing materials in the earlier discharges leads to a moderate reduction in Z_{eff} in later plasmas which can be interpreted as evidence of a conditioning effect. We note that we are limiting this analysis to the period from 7 – 10s to avoid any complications which may arise during discharge onset. For example, there is a general increase in Z^{eff} which appears at t = 3s only for WEST 58059, we believe that this is result of a mobilization of some material at the onset of the LH system, and it then takes multiple seconds for

the value to decay down to the roughly steady state value observed just before the injection of powder at t = 10s.

Panel c), displays the post injection period which also demonstrates that for the latter discharges (WEST 58053 & WEST 58059), where substantial material is injected, there are slightly reduced values of the Z_{eff} baseline observed after the conclusion of the injections. Again demonstrating the ability of the injected material to condition the machine within a discharge.

As can be expected, and is shown in panel d) of figure 7, Z_{eff} increases as the quantity of powder is increased from a non-injection level of 1.6 to a value just over 3 for an injection rate of 54mg/s this corresponds to an introduction of $3x10^{21}$ B atoms/s. Given that $n_e = 4x10^{19}$ m^{-2} this presents a lower bound of $n_D = 2x10^{19}$ m^{-2} and $n_B = 4x10^{18}$ m^{-2}. Thus, for this section of the discharge we estimate that B atoms represent 16% of the concentration but 50% of the charge balance, a substantial dilution of the main ion species.

IV.3 Effects upon radiated power with increasing powder injection levels

Powder injections have a stark and yet sometimes counterintuitive effect upon global radiated power as shown in Figure 8. The top panel shows the initial baseline discharge (WEST 58049), which did not involve substantial powder injection and as such the radiated power level remains constant throughout the LH heated portion of the discharge. As seen in panel b), the introduction of powder now becomes evident in an increase in radiated power. This is similar to corresponding increases seen in the boron spectroscopy as seen in panel b) of figure 2 earlier in the manuscript. We note however that as the quantity of injected material increases the direct correlation between it and the radiated power starts to deviate. During WEST 58051, shown in panel c), we note that while the level of radiated power does significantly increase as B is introduced it does not continue to increase as the quantity of powder is further amplified, in fact, after peaking at t = 14s, the radiated power rolls over and decreases throughout the remainder of the injection period despite increases in the injected powder level from 14 mg/s to 43 mg/s at the highest level and contrary to what is shown on the spectroscopic and visible diagnostics shown in the equivalent panel c) in figure 2. The behavior of the radiated power again tracks closely with the injected powder quantity during WEST 58053 (panel d) as a reduction of injection level from 20mg/s to 14mg/s at t = 15s does indeed result in a matching decay of the radiated power level. This is in stark contrast to the behavior evidenced during WEST 58059. This discharge started with an injection rate of 20mg/s from 10-12.5s and then increased to 34mg/s from 12.5-15s. During this increase the radiated power as can be seen in panel e) the radiated power level gain was slightly reduced similar to what was observed in WEST 58051. However, as the powder injection level is further increased to 54 mg/s there is a sharp decrease in the radiated power level which is maintained throughout the injection period. Then, during the final injection period from 17.5-20s, when the injection rate is reduced back to 20mg/s, the radiated power is observed to increase back to its previous level. This is again in contrast to the

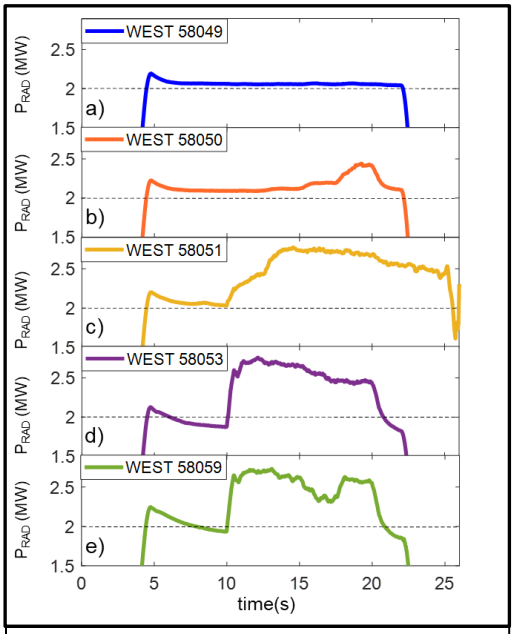

Figure 8 : Radiated power response to powder injection. The black dashed guideline at 2MW is used to aid resolution of shot-to-shot changes in the pre-injection period

decrease in powder throughput as observed through the visible camera, boron spectroscopy and Z_{eff} measurements. We believe these changes in the radiated power which are contrary to the level of injected boron are due to the noted ability for powder injection to flush higher Z core impurities as has been demonstrated on DIII-D[27]. The extent to which this is occurring in WEST will be the subject of further experiments and analysis.

As a final observation about the radiated power, we note that after a plasma with significant powder injection, that the pre-injection portion of the discharge displays radiated power levels which are reduced from the previous baseline level, again suggesting a conditioning effect provided by the boron powder. This is evidenced by the radiated power in the pre-injection periods of panels d) and e) dropping below the dotted lines in the respective panels of figure 8 which show the 2MW level.

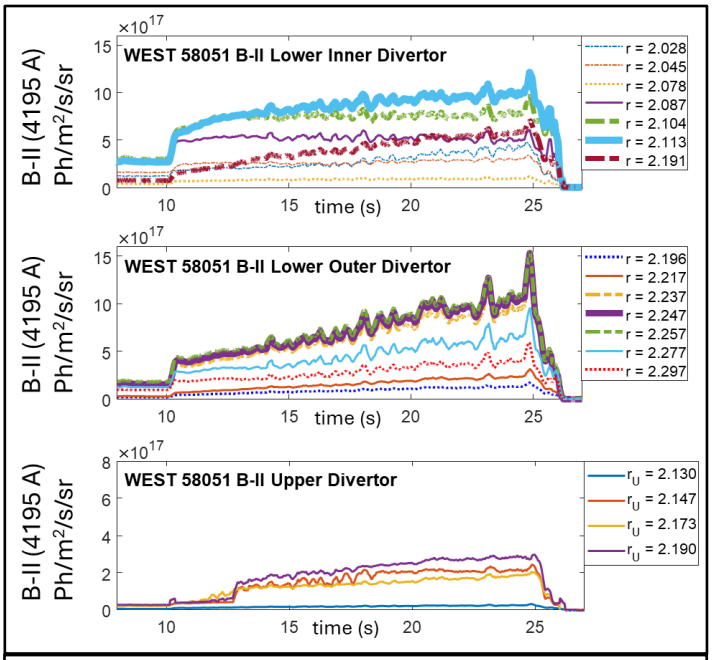

Figure 9 : Boron transport to the upper and lower divertor surfaces during lower single null WEST plasmas. Lower divertor spectroscopy channels arranged by increasing radius and line thickness is indicative of the distance from the inner and outer strike points respectively.

IV.4 Boron Transport to Limiter and Divertor surfaces

The utilization of the Impurity Powder Dropper as an in-situ conditioning method depends upon the ability of the injected material to be transported to the locations where the conditioning is needed, namely the limiter and divertor surfaces. To that end we examine the intensity of B-II emissions at various surfaces throughout the WEST device for WEST 58051. We chose this particular discharge as the ramping of the boron rate throughout the injection period allows us to examine not only the presence or absence of boron at these various limiting surfaces, but also the response to elevating injection rates over an extended period of deposition. Boron signals at the divertor surfaces are displayed in figure 9. As can be seen, boron levels at the lower divertor (top and middle panels) increase sharply at t=10s coincident with the initiation of the boron injection with the most abrupt increase occurring at the lower inner divertor. This is consistent with camera observations and recent simulations[28, 29] that the initial powder assimilation appears to travel over the crown of the discharge and down through the high field side. However, we note that the boron levels on the high field side divertor, while they do increase do not appear to do so at a level commensurate with the increase in powder level. As shown, the signal traces at the outer divertor all consistently increase under elevated powder injection levels while only a subset of chords behave this way at the inner divertor. These signals are then also contrasted with the signatures observed at the upper divertor. The powder injection series of discharges was conducted in a lower single null magnetic configuration, so the majority of the particle flux is directed to the bottom of the vessel. Irrespective though, it is interesting to note that the boron level at the upper divertor does not begin to accumulate until the second injection period at t = 12.5s It may be that

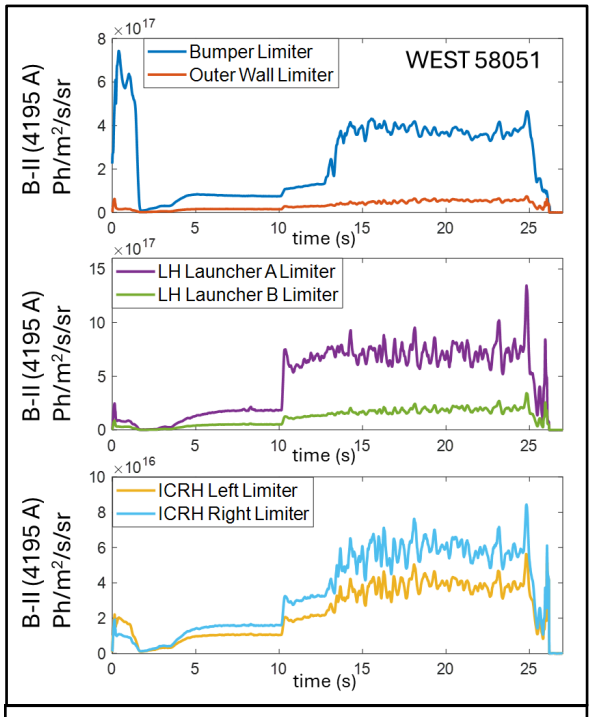

Figure 10 : Boron transport to limiter surfaces. The signal traces above represent the average behavior of multi-chord measurements at the corresponding limiters. Note that during these discharges the Bumper Limiter was comprised of BN tiles which encountered heavy plasma contact during startup.

there is a powder injection threshold beyond which elevated injections lead to increases in the quantity of material sputtered from the lower divertor and redistributed throughout the vessel.

Boron transport is also evidenced in spectroscopic signals gathered at the WEST limiter surfaces. In figure 10 we show the average response at the Inner and Outer limiters (top) as well as at the Lower Hybrid (LH) (middle) and Ion Cyclotron Resonant Heating (ICRH) (bottom) limiters. Note that the large signal seen during the initiation of the plasma pulse is due to the Bumper limiter tiles being comprised of Boron Nitride and not due to any powder injection by the IPD. Much like the divertor we can see first evidence of prompt deposition on surfaces magnetically close to the IPD injection point. Thus, there is a noted upswell in boron signal at the LH limiter coincident with the first introductions of B powder at 10s, however the boron level quickly saturates and does not appreciably increase beyond this despite the fact that the boron injection rate quadruples from 10mg/s at 10-12.5s to over 40mg/s during the 22.5-25s period. The other limiter surfaces show a strong increase in the boron signal after the subsequent injection step at 12.5s, but then these traces also show a rapid saturation and do not ramp commensurate with the continued increase in B injection rate. We postulate that this behavior is more indicative of the sputtering rate from the edge plasma contact and thus can be viewed as evidence of layer formation as the spectroscopic signal only resolves the boron in the near surface layers of the plasma, thus any additional boron being delivered would be adherent to the surface where it will not be resolved by the spectroscopic diagnostic. Just such layer formation as a result of multiple B powder injection discharges has been observed in AUG[30] with a correlation between the injection quantity and layer thickness determined. Further examination of this effect will be explored in future experiments through the utilization of edge collector probes and depositional coupons.

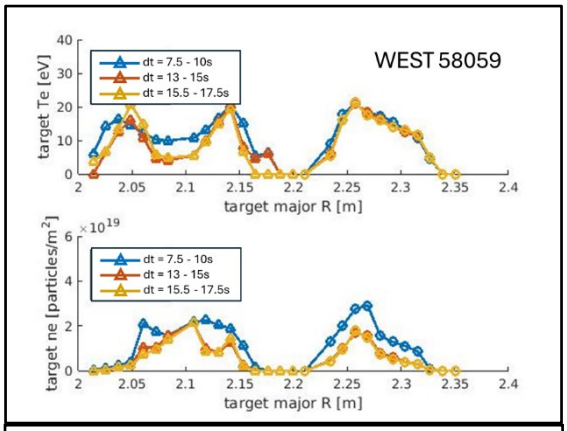

Figure 11 : Lower divertor Langmuir probe measurements during powder injection. The first time period is prior to any powder injection while the second and third are during periods of 34 mg/s and 54 mg/s respectively.

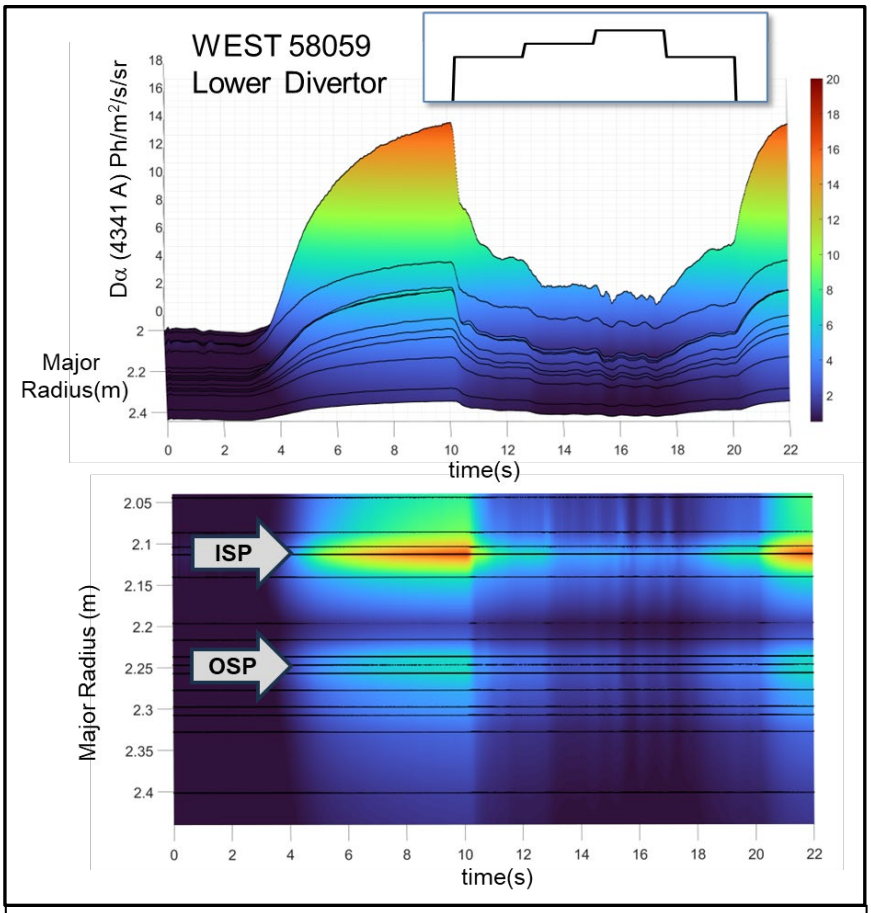

Figure 12 : Response of divertor Dα signals to boron powder injection. Multiple views of a 3D plot of the Dα response to powder injection at the lower divertor is shown. The top panel shows a temporal evolution of the Dα levels at the lower divertor with the color bar having the same units as the vertical scale added to help resolve scale, while the bottom panel displays a top-down image with the same color scale. Arrows indicate the inner(ISP) and outer strike point(OSP), and the black lines denote spectroscopy chord locations. Inset graph displays above the top panel shows the IPD voltage settings for this discharge

As noted, the divertor response to the injection of boron containing impurities is prompt and substantial, and yet examining the Langmuir probe measurements for boron injection discharges as shown in figure 11, we can see that the divertor density remains relatively unchanged. Thus, there must be a subsequent reduction in the main ion species in order to maintain the near constant density. As can be seen in figure 12, the level of divertor Dα light is substantially diminished as

a result of the powder injection. This reduction in the signal level is proportional to the powder injection rate, observable by comparing the inset graph of the IPD excitation voltage with the attenuation of the signal. While it would seem reasonable to attribute this decrease primarily to main ion dilution, an examination of the gas fill rates for this discharge (WEST 58059) when compared to the control discharge (WEST 58049), as is done in figure 13, shows that there is actually a substantially higher fill rate despite the fact that there is a large quantity of additional material being introduced and thus contributing to the electron fraction. As such, we conclude that the reduction in Dα is most likely indicative of an elevated level of codeposition as well as a substantial reduction in recycling due to gettering provided by the newly deposited boron layer. This presents a concern for the utilization of real-time wall conditioning in future fusion reactors as the fuel component Tritium is a rare and highly controlled substance and having it trapped as an adsorbed gas within the wall coatings, either through B powder introduction or GDB, is not an effective or efficient use of the available inventory.

Experiments undertaken at AUG[30] showed the efficacy of boron powder in generating layer formation within the deposition dominated areas was roughly 10 times higher than in a typical GDB, however the coverage area is limited to the plasma wetted surfaces. This is a noted difference from the volume breakdown method of GDB which provides a more uniform surface coverage and thus an extended period of impurity control. This was confirmed during experiments on LHD, where it was observed that real time IPD type boronization injections worked well to reduce impurity content, specifically oxygen, during extreme long pulse discharges ($t > 200s$). However, these effects were limited in duration after the conclusion of the discharge while the conditioning effects observed from a standard GDB lasted for the full run campaign. All this being said, the issue of dust generation and fuel retention remain an area of concern. Solutions such as active dust collection mechanisms as well as elevated temperatures to desorb the Tritium have been proposed, but a final practical solution remains to be developed..

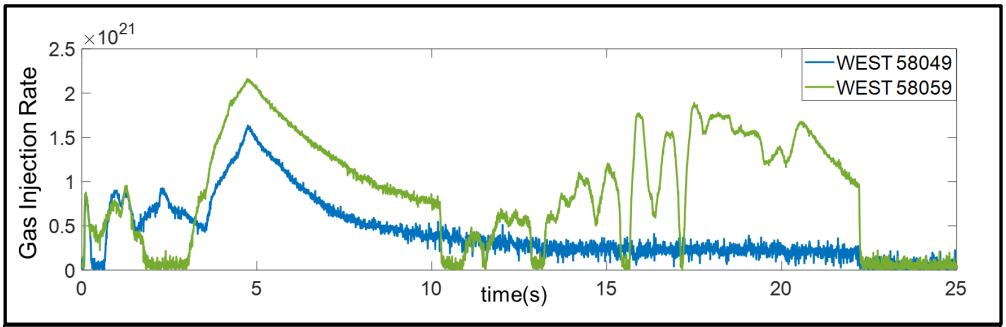

Figure 13 : Comparison of gas injection rates for discharges without(WEST 58049) and with (WEST 58059) boron injection

CONCLUSION

The utilization of an impurity powder dropper on WEST, initially installed to maintain premium wall conditions during long pulse discharges, has demonstrated the ability to enhance the performance of plasma operations. Through a series of stepped injections, the ability of powder to provide sustained increases to the neutron rate (N_n) by up to 200%, the electron temperature(T_e) by up to 35% and the stored energy (W_{MHD}) by up to 18% have all been observed. In addition, these increases are sustainable over multiple confinement times and only appear to be limited by the duration of powder injection. While not confirmed on WEST these enhancements are consistent with turbulence reduction through profile modification as well as main ion dilution as seen on other devices. In addition, the ability for the material introduced by the IPD to be deposited on a full range of limiter and diverter surfaces throughout the toroidal extent of the vacuum vessel provides confidence that the employment of a single actuator can be utilized to distribute conditioning material to a substantial fraction of the plasma-wetted areas. Further experiments are required to expand the understanding of IPD applicability, and as such, upcoming programs will be utilized to inject boron powder in quantities comparable to those used in standard GDB, enabling an assessment of impurity concentration changes due to active conditioning over long-pulse timescales. Additional studies will also examine the duration of conditioning effects and the compatibility of material injection with extended plasma operation. These findings will guide future experiments in which the IPD could be used to provide active feedback for long-pulse discharges.

Declaration of competing interest

The authors declare that they have no known competing financial interests or personal relationships that could have appeared to influence the work reported in this paper.

Data availability

Data will be made available on request.

Acknowledgements

This material is based upon work supported by the U.S. Department of Energy, Fusion Energy Sciences in the Office of Science under Awards DE-AC02-09CH11466 (PPPL) and DE-AC05-00OR22725 (ORNL). The United States Government retains a non-exclusive, paid-up, irrevocable, world-wide license to publish or reproduce the published form of this manuscript, or allow others to do so, for United States Government purposes.

Disclaimer

Bibliography

[1] F. Romanelli, et al., 2015 Nucl. Fusion 55 104001

[2] C. Giroud, et al., 2013 Nucl. Fusion 53 113025

[3] D. K. Mansfield, et al., 2001 Nucl. Fusion 41 1823

[4] R. Maingi, et al., 2012 Nucl. Fusion 52 083001

[5] T. H. Osborne, et al., 2015 Nucl. Fusion 55 063018

[6] A. Bortolon, et al., 2019 Nucl. Mater. Energy 19 384-389

[7] R. Lunsford, et al., 2019 Nucl. Fusion 59 126034

[8] Z. Sun, et al., 2021 Phys. Plasmas 28 082512

[9] R. Lunsford, et al., 2022 Nucl. Fusion 62 086021

[10] F. Nespoli, et al., 2022 Nature Physics 18 350-356

[11] R. Lunsford, et al., 2021 Phys Plasmas 28 082506

[12] J. Bucalossi, et al., 2024 Nucl. Fusion 64 112022

[13] C. Bourdelle, et al., 2015 Nucl. Fusion 55 063017

[14] M. Missirlian, et al., 2023 Fusion Eng. and Des. 193 113683

[15] J. Bucalossi, et al., 2022 Nucl. Fusion 62 042007

[16] A. Gallo, et al., 2024 Nucl. Mater. Energy 41 101741

[17] G. Bodner, et al., 2022 Nucl. Fusion 62 086020

[18] A. Nagy, et al., 2018 Rev. Sci. Instrum. 89 10K121

[19] Z. Sun et al., 2019 Nucl. Mater. Energy 19 124

[20] E. P. Gilson, et al., 2021 Nucl. Mater. Energy 28 101043

[21] F. Effenberg, et al., 2022 Nucl. Fusion 62 106015

[22] A. Bortolon, et al., 2020 Nucl. Fusion 60 126010

[23] G. Bodner, et al., 2024 Plasma Phys. Control Fusion 66 045022

[24] K. Afonin, et al., 2024 Nucl. Mater. Energy 40 101724

[25] N. Fedorczak, et al., 2024 Nucl. Mater. Energy 41 101758

[26] R. Lunsford, et al., 2024 Nucl. Mater. Energy 40 101726

[27] R. Lunsford, et al., IAEA 2021 “The impact of low-z powder injection on intrinsic impurities in DIII-D” Preprint submitted : 2020 IAEA Fusion Energy Conference, Nice (2021)

28th IAEA Fusion Energy Conference (FEC 2020) Contribution ID: 811

[28] K. Afonin et al., 2023 Nucl. Fusion 63 126057

[29] F. Effenberg et al., 2025 Nucl Mater. Energy 42 101832

[30] K. Krieger et al., 2023 Nucl. Mater. Energy 34 101374

[31] S. Masuzaki et al., 2025 Nucl. Mater. Energy 42 101843